J Sol-Gel Sci Technol (2017) 81:59–68
DOI 10.1007/s10971-016-4272-0

ORIGINAL PAPER: NANO- AND MACROPOROUS MATERIALS (AEROGELS, XEROGELS, CRYOGELS, ETC.)

Ethylene polymerization and hydrodechlorination of 1,2-dichloroethane mediated by nickel(II) covalently anchored to silica xerogels

Julien G. Mahy[1] · Vincent Claude[1] · Luigi Sacco[2] · Stéphanie D. Lambert[1]

Received: 1 March 2016 / Accepted: 21 November 2016 / Published online: 15 December 2016

Abstract Ni/SiO_2 cogelled xerogel catalysts have been prepared in ethanol containing nickel acetylacetonate, tetraethoxysilane (TEOS), an aqueous ammonia solution of 0.54 mol L^{-1} and either a commercial sylilated ligand, *3*-(*2*-aminoethyl)aminopropyltrimethoxysilane (EDAPMS), or a home-made new silylated pyrazolypyridine ligands, respectively *2*-[*4*-[*3*-(trimethoxysilyl)propyl]-*3*,*5*-dimethyl-*1H*-pyrazol-1-yl]pyridine (MS-PzPy) and *2*-[*4*-[*3*-(trimethoxysilyl) propyl]-*3*,*5*-dimethyl-*1H*-pyrazol-1-yl]-*6*-methylpyridine (MS-PzPyMe), able to form a chelate with a metal ion such as Ni^{2+}. All samples form homogeneous and very highly dispersed Ni/SiO_2 cogelled xerogel catalysts. The resulting catalysts are composed of nickel nanoparticles with a diameter of about 2.8 nm, located inside primary silica particles exhibiting a monodisperse microporous distribution. The silylated organic ligand has a strong influence on the textural properties of cogelled xerogel catalysts, both before and after calcination and reduction steps. Changing the nature of the silylated ligand permits tailoring textural properties such as pore volume, pore size and surface area. Homogenous nickel complexes synthesized from pyrazolylpyridine derivatives are inactive for ethylene polymerization. In opposite, heterogenous nickel-based catalysts onto silica xerogel synthesized from pyrazolylpyridine derivatives bearing a tethered trialkoxysilyl group allow increasing ethylene polymerization activity. Although nickel nanoparticles are located inside the silica crystallites, their complete accessibility, via the micropore network, has been shown. For *1,2*-dichloroethane hydrodechlorination over Ni/SiO_2 catalysts, the conversion of *1,2*-dichloroethane is high at the temperature of 350 °C and mainly ethane is produced.

Graphical Abstract

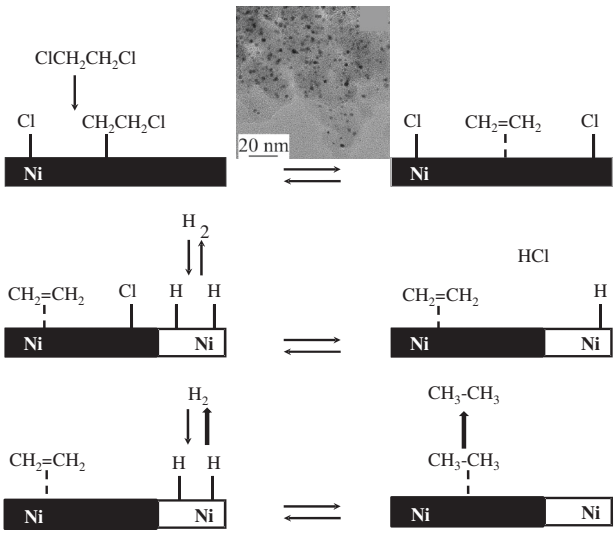

Keywords Silylated ligand · Covalently attached Ni complexes · Cogelled xerogel catalyts · Ethylene polymerization · Hydrodechlorination

✉ Stéphanie D. Lambert
stephanie.lambert@ulg.ac.be

[1] Department of Chemical Engineering—Nanomaterials, Catalysis and Electrochemistry, B6a, University of Liège, Liège B-4000, Belgium

[2] Laboratory of Macromolecular Chemistry and Organic Catalysis (CERM), B6a, University of Liège, Liège B-4000, Belgium

1 Introduction

Heterogeneous catalysis is widely used for industrial applications thanks to the well-known advantages of easier product–catalyst separation and recovery of the catalyst process and, often, to the enhanced stability of the catalyst. But in terms of selectivity, homogeneous catalysis usually provides better results. From this point of view, the grafting of homogeneous catalysts onto a solid support seems the ideal combination in order to achieve the advantages of both heterogeneous and homogeneous catalysis, allowing the developing of more environmentally friendly and economical processes with potential application in the industry [1, 2]. Further, to covalently link a homogeneous onto silica (a support which is thermally, chemically, and mechanically resistant with a well defined structure) is the best way to limit metal leaching and sintering.

It is known that the activity of immobilized molecular catalysts may be remarkably affected by the nature of the support. It is apparent that development of heterogeneous processes relies on our ability to design diverse and specifically customized support materials. From this point of view, sol–gel chemistry is a versatile route to tailored organically-modified silica. This process is based on the hydrolysis and condensation of monomeric precursors—typically silicon alkoxides—leading to the formation of the 3-dimensional porous network [3]. According to the cogelation sol-gel process proposed by Schubert et al. [4] and Lambert et al. [5–8] used this method to synthesize metallic oxide, mono-and bimetallic cogelled xerogel catalysts. Further thermal treatments of cogelled xerogel catalysts gave highly dispersed palladium, silver, nickel, copper or iron oxide nanoparticules in Pd/SiO_2, Ni/SiO_2, Ag/SiO_2, Cu/SiO_2 or Fe-based catalysts and alloy nanoparticles in $Pd\text{-}Ag/SiO_2$, $Pd\text{-}Cu/SiO_2$ and $Ni\text{-}Cu/SiO_2$ catalysts. Furthermore, in all metallic cogelled xerogel catalysts, the complete accessibility and activity of the metallic sites through the microporous network were experimentally established and verified in a typical heterogeneous gaseous reaction, the catalytic hydrodechlorination of *1,2*-dichloroethane, an important reaction for the treatment of chlorinated industrial wastes [5–7]. Finally, it has been shown [7] that the very particular structure of those catalysts allows to avoid diffusional limitations. Indeed, in xerogel catalysts, in order to reach active sites, reactants must first diffuse through large pores located between aggregates of SiO_2 particles and then through smaller pores between those elementary particles inside the aggregates. Finally, they diffuse through micropores inside the silica particles. It was shown that there is no problem of mass transfer at each of the three levels [7]. The Weisz modulus, which compares the observed reaction rate to the diffusion rate, has a value much smaller than 1 at three discrete levels: (i) macroscopic pellet, (ii) aggregate of silica particles, (iii) elementary silica particle containing an active metallic crystallite. So there are no pore diffusion limitations in gaseous phase [7].

In last decade, nitrogen-based ligands containing one of several Schiff bases have been reported to form active catalysts with "late-metal" (such as Fe, Pd, Ni,…) for the ethylene polymerization [9–12]. Moreover, substituted pyrazole-based organometallic complexes gave also promising results in this field [12–14]. These facts let us suggest that the pyrazolylpyridine derivatives bearing a tethered trimethoxysilylated group synthesized in a previous work [15] are potentially good candidate to prepare hybrid catalyst (i.e., soluble organometallic complexes covalently bonded onto an insoluble support, in this case silica) with Ni-II, Fe-II or Pd-II for ethylene polymerization. Indeed, recently, works have been realized to graft Ni- [16–18], Ti- [19], Zr- [19] or Fe- [18, 19] complexes on different supports like silica [19], carbon nanotubes [16] or mica [17, 18] to enhance ethylene polymerization. In these studies, results show that the molecular structure of these complexes was maintained after grafting and evidenced the beneficial influence of the support. Furthermore, Nandi et al. [20] showed that functionalized mesoporous silica supported copper (II) and nickel (II) catalysts were very active towards the selective epoxidation of olefins like cyclohexene, *trans*-stilbene, styrene, α-methyl styrene, cyclooctene and norbornene in the presence of *tert*-butyl hydroperoxide oxidant under mild liquid phase reaction conditions. So heterogenized systems are more active than the corresponding homogeneous catalysts [16, 20].

In this study, the heterogenization of nickel(II) acetate acetylacetonate *via* a sol-gel process mediated by three following ligands was described : (i) one commercial ligand, *3-(2*-aminoethylamino)propyltrimethoxysilane and (ii) two home-made ligands : *2*-[*4*-[*3*-(trimethoxysilyl)propyl]-*3,5*-dimethyl-*1H*-pyrazol-*1*-yl]pyridine (MS-PzPy) and *2*-[*4*-[*3*-(trimethoxysilyl)propyl]-*3,5*-dimethyl-*1H*-pyrazol-*1*-yl]-*6*-methylpyridine (MS-PzPyMe). All these hybrid organic-inorganic materials were characterized to determine their textural properties, the size and the dispersion of Ni particles and tested in different reactions such as ethylene polymerization and hydrodechlorination of *1,2*-dichloroethane.

2 Experimental section

2.1 Synthesis of pyrazolylpyridine ligands

Pyrazolylpyridine ligands, namely *2*-(*3,5*-dimethylpyrazol-*1*-yl)pyridine (MS-PzPy) and *2*-(*3,5*-dimethyl-*1H*-pyrazol-*1*-yl)-*6*-methylpyridine (MS-PzPyMe) are synthesized from

Fig. 1 Structure and characterization of pyrazolylpyridine derivatives

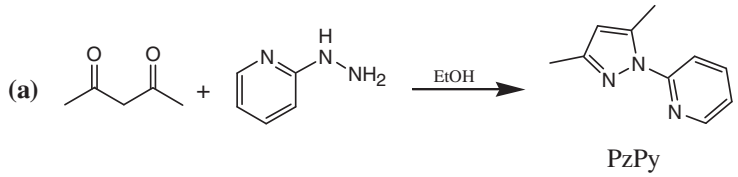

2-(3,5-dimethylpyrazol-1-yl)-pyridine, PzPy
NMR 400 MHz ($CDCl_3$)
^1H : δ = 2.28 (s, 3H), 2.61 (s, 3H), 5.97 (s, 1H), 7.11 (m,1H), 7.74 (m, 1H), 7.82 (m, 1H), 8.39 (m, 1H).

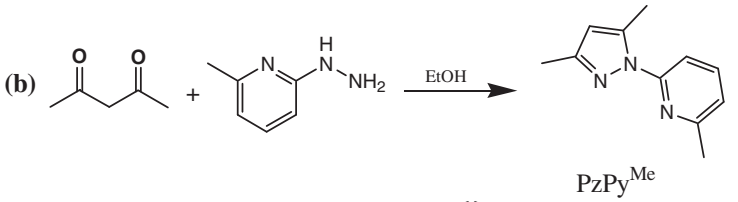

2-(3,5-dimethylpyrazol-1-yl)-6-methylpyridine, $PzPy^{Me}$
NMR 400 MHz ($CDCl_3$)
^1H : δ = 2.28 (s, 3H), 2.50 (s, 3H), 2.60 (s, 3H), 5.95 (s, 1H), 6.96 (m, 1H), 7.60 (m, 2H).

Table 1 Properties of organometallic complexes and ethylene consumption

Complex	Complex color	IR absorptions of C–N bonds (cm^{-1})	Ethylene consumption (mol)
$NiBr_2(PzPy)$	light green	1605, 1579, 1563	0.09
$NiBr_2(PzPy^{Me})$	orange (pink in CH_2Cl_2)	1612, 1575, 1566	0.03

acetylacetone, *3,5*-heptanedione, *2*-hydrazinopyridine or *2*-hydrazino-*6*-methylpyridine, as described in [15]. The synthesis and ^1H NMR spectra of pyrazolylpyridine derivatives are presented in Fig. 1.

2.2 Synthesis of homogeneous nickel complexes of pyrazolylpyridine derivatives

Nickel complexes of pyrazolylpyridine derivatives, $NiBr_2(PzPy)$ and $NiBr_2(PzPy^{Me})$ are generated in dichloromethane by addition of the metal salt to a solution of the ligand. So a suspension of 10^{-5} mol of nickel(II) bromure and 1.1×10^{-5} mol of pyrazolylpyridine ligand in 0.4 ml of dichloromethane are stirred for 30 min under an anhydrous argon atmosphere. The properties of these organometallic complexes are presented in Table 1.

2.3 Synthesis of heterogeneous Ni/SiO_2 cogelled xerogel catalysts

Three Ni/SiO2 xerogel cogelled catalysts with 1 wt.% of nickel were prepared from three silylated ligands. Each catalyst is named by the corresponding silylated ligand used: *3*-(*2*-aminoethylamino)propyltrimethoxysilane (NH_2-$(CH_2)_2$-NH-$(CH_2)_3$-Si$(OCH_3)_3$ or EDAPMS, commercial product, Sigma-Aldrichs), *2*-[*4*-[*3*-(trimethoxysilyl) propyl]-*3*,*5*-dimethyl-*1H*-pyrazol-*1*-yl]pyridine (MS-PzPy, synthesis described in [15]) and *2*-[*4*-[*3*-(trimethoxysilyl) propyl]-*3,5*-dimethyl-*1H*-pyrazol-*1*-yl]-*6*-methylpyridine (MS-PzPyMe, synthesis described in [15]). The last two ligands are pyrazolylpyridine derivatives bearing a tethered trialkoxysilyl group and their structure is presented in Fig. 2. 4.6×10^{-4} mol of nickel(II) acetylacetonate (Ni $[CH_3COCH{=}C(O\text{-})CH_3]_2{=}Ni(acac)_2$) is dissolved for 60 min in 13 ml of absolute ethanol containing 9.3×10^{-4} mol of either EDAPMS, MS-PzPy or MS-PzPyMe. After the addition of 9.75 ml of tetraethylorthosilicate (Si $(OC_2H_5)_4$ = TEOS), 4.0 ml of 0.54 N NH_3 aqueous solution in 13 ml of absolute ethanol is added with vigorous stirring. The vessel is then tightly closed and heated up to 80 °C for 72 h (gelling and aging [3]). The wet gels were dried under vacuum according to the following procedure : the flasks were opened and put into a drying oven at 80 °C, and the pressure was slowly decreased (to prevent gel bursting) to reach the minimum value of 1200 Pa after 90 h. The drying oven was then heated at 150 °C for 72 h. The resulting samples are xerogels [3]. The conditions of calcination are as follows: the three samples are heated up to 400 °C at a rate of 120 °C h^{-1} under flowing air (0.02 mmol s^{-1}); this temperature is maintained for 12 h in air (0.1 mmol s^{-1}). For the reduction, samples are heated up to 500 °C at a rate of 500 °C h^{-1} under flowing H_2 (0.23 mmol s^{-1}) and maintained at this temperature for 3 h (same flow).

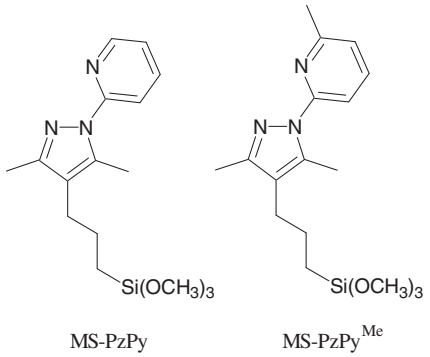

Fig. 2 Structure of pyrazolylpyridine derivatives bearing a tethered trimethoxysil group

2.4 Characterization of heterogeneous Ni/SiO_2 cogelled xerogel catalysts

Real nickel contents in Ni/SiO_2 cogelled xerogel catalysts were measured from inductively coupled plasma atomic emission spectroscopy (ICP-AES) on a Spectroflam from Spectro Analytical Instruments. Samples were dissolved in concentrated acids (18M H_2SO_4, 22M HF, 14M HNO_3). Nickel contents were obtained by comparison with standard solutions in the same medium.

Nitrogen adsorption-desorption isotherms were measured at 77 K on a Fisons Sorptomatic 1990 after outgassing for 24 h at ambient temperature. After a 2 h outgassing at ambient temperature, Hg porosimetry measurements were performed with sample monoliths using a manual porosimeter from 0.01 to 0.1 MPa and a Carlo Erba Porosimeter 2000 from 0.1 to 200 MPa.

Ni particles sizes were examined by transmission electron microscopy (TEM) with a Philips CM100 microscope. All samples were impregnated with an epoxy resin (EPON 812) to which an amine was added to serve as a hardener. Hardening goes on for 72 h at 60 °C and 60 nm slices were then cut up with a Reichert-Jung Ultracut E microtome. Finally, these slices were put on a copper grid.

Nickel dispersion in heterogeneous Ni/SiO2 xerogel cogelled catalysts was determined from H_2 chemisorption at 30 °C on a Fisons Sorptomatic 1990 device. Before measurements, the calcined sample was reduced in situ in flowing H_2 (0.003 mmol s^{-1}) at 500 °C for 3 h. After, this sample was outgassed under vacuum at 450 °C for 16 h. A double adsorption method was used : (i) first adsorption isotherm was measured, which includes both physisorption and chemisorption ; (ii) after a 30 min outgassing at 30 °C, a second isotherm was measured which includes physisorption only. Both isotherms are determined in the pressure range of 10^{-8}–2 10^{-1} kPa. The difference between first and second isotherms gave the H_2 chemisorption isotherm [21–23].

2.5 Catalytic experiments

2.5.1 Ethylene polymerization

Homogeneous nickel complexes of pyrazolylpyridine derivatives are tested for ethylene polymerization in toluene in the presence of methylaluminoxane (MAO) as cocatalyst. Experimental conditions are the following: 30 ml of toluene, ambient temperature, MAO/metal = 700, 10^{-5} mol of complexe, polymerization time = 1 h; ethylene pressure = 1 MPa.

Heterogeneous dried Ni/SiO_2 cogelled xerogel catalysts are crushed, sieved between 250 and 500 µm and tested for ethylene polymerization with the same experimental conditions than these one for homogeneous catalysts.

2.5.2 1,2-Dichloroethane hydrodechlorination on heterogeneous Ni/SiO_2 cogelled xerogel catalysts

0.15 g of samples EDAPMS, MS-PzPy and MS-PzPyMe are crushed, sieved between 250 and 500 µm and tested for *1,2*-dichloroethane hydrodechlorination, which was conducted in a stainless steel tubular reactor (internal diameter: 10 mm) at a pressure of 0.3 MPa. The reactor was placed in a convection oven. A constant flow of each reactant was maintained by a Gilson piston pump for $ClCH_2$-CH_2Cl and Brooks mass flow controllers for H_2 and He. The effluent was analyzed by gas chromatography (ThermoFinnigan with FID) using a Porapak Q5 packed column. Prior to each experiment, each calcined Ni/SiO_2 xerogel cogelled catalyst was reduced in situ at atmospheric pressure in flowing H_2 (0.023 mmol s^{-1}) while being heated to 400 °C at a rate of 350 °C/h and was maintained at this temperature for 4 h. After reduction, each Ni/SiO_2 catalyst was cooled in H_2 to the desired initial reaction temperature of 200 °C. The total flow of the reactant mixture was 0.45 mmol s^{-1} and consisted of $ClCH_2$-CH_2Cl (0.011 mmol s^{-1}), H_2 (0.023 mmol s^{-1}), and He (0.42 mmol s^{-1}). The temperature was successively kept at 200 °C (2 h), 250 °C (2 h), 300 °C (2 h), 350 °C (2 h) and 300 °C (4 h). The effluent was analyzed every 15 min and eight analyses were made at each temperature (60 for the last level).

3 Results and discussion

3.1 Textural properties of heterogeneous Ni/SiO_2 xerogel cogelled catalysts

Textural properties are presented in Table 2 both for samples after vacuum drying step (the sample names are followed by the word “dried” in Table 2) and for the same samples after vacuum drying, calcination, and reduction

Table 2 Textural properties, nickel average particle size and catalytic activity for Ni/SiO_2 xerogel cogelled catalysts

Sample	S_{BET} ($m^2\,g^{-1}$)	V_v ($cm^3\,g^{-1}$)	TEM		Chemisorption		Mass of polyethylene (g)			
			d_{TEM} (nm)	σ_{TEM} (nm)	D (%)	d_{chem} (nm)				
EDAPMS dried	145	2.3	–[a]	–[a]	–[a]	–[a]	0.085			
MS-PzPy dried	230	1.8	–[a]	–[a]	–[a]	–[a]	0.105			
MS-PzPyMe dried	290	1.7	–[a]	–[a]	–[a]	–[a]	0.520			
							r (mmol s^{-1} kg_{Ni}^{-1})		TOF (s^{-1})	
							300 °C	350 °C	300 °C	350 °C
EDAPMS	300	2.9	2.7	0.4	34	3.0	105	690	0.02	0.12
MS-PzPy	390	2.0	2.9	0.3	32	3.1	105	680	0.02	0.12
MS-PzPyMe	420	1.8	2.8	0.2	34	2.9	110	680	0.02	0.12

S_{BET} specific surface area obtained by BET method, V_v total cumulative specific pore volume, d_{TEM} mean diameter of Ni particles measured by TEM, σ_{TEM} standard deviation associated with d_{TEM}, D Ni dispersion measured by H_2 chemisortpion, d_{chem} mean diameter of Ni particles derived from dispersion D, r specific consumption rate of *1,2*-dichloroethane, *TOF* turnover frequency

[a] not measured

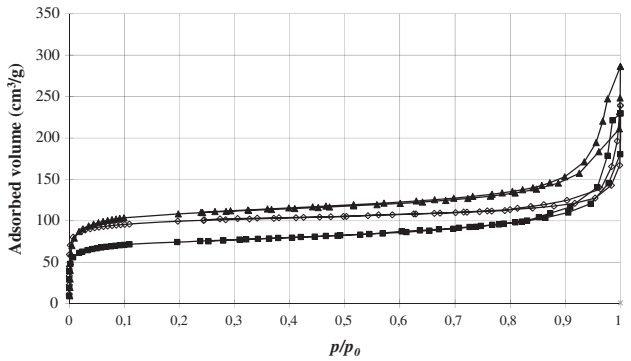

Fig. 3 Nitrogen adsorption-desorption isotherms of samples EDAPMS (■), MS-PzPy (◊) and MS-PzPyMe (▲)

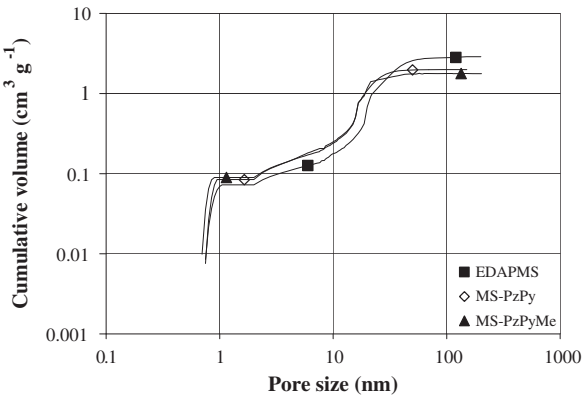

Fig. 4 Pore size distributions of samples EDAPMS (■), MS-PzPy (◊) and MS-PzPyMe (▲)

steps. The specific surface area obtained from the BET method, S_{BET}, and the total cumulative specific pore volume, V_v, that is, the pore volume obtained by addition of pore volume measured by mercury porosimetry (width < 7.5 nm) and cumulative volume of micropores and mesopores of widths between 2 and 7.5 nm measured by nitrogen adsorption–desorption, increase when dried Ni/SiO_2 xerogel cogelled catalysts are calcined and reduced.

Figure 3 shows the nitrogen adsorption-desorption isotherms for Ni/SiO_2 cogelled xerogel catalysts after calcination and reduction steps. These isotherms are characteristic of microporous and mesoporous materials [24]: (i) at low relative pressure, a sharp increase of the adsorbed volume is followed by a plateau, which corresponds to type I isotherm according to BDDT classification [24], which is characteristic of microporous adsorbents; (ii) all samples exhibit a narrow adsorption-desorption hysteresis loop for p/p_0 values close to 1 and this hysteresis is characteristic of capillary condensation in large mesopores.

Figure 4 shows the evolution of the cumulative volume distributions over the entire pore size range for Ni/SiO_2 cogelled xerogel catalysts after calcination and reduction steps. These curves were obtained by applying a combination of various methods to their respective validity domains and by adding the porous volume distributions corresponding to each domain [5]. All samples are characterized by a steep volume increase around 0.8 nm, followed by a plateau. This plateau, characteristic of micropores volume, slightly increases from 0.07 $cm^3\,g^{-1}$ for EDAPMS to 0.09 $cm^3\,g^{-1}$ for MS-PzPyMe. Furthermore, in the range of mesopores (2 nm < width < 50 nm), samples MS-PzPy and MS-PzPyMe present slightly higher volumes than sample EDAPMS. These both observations are in correlation with the increase of S_{BET} (Table 2) from 300 $m^2\,g^{-1}$ for sample EDAPMS to 390 and 420 $m^2\,g^{-1}$ for MS-PzPy and MS-PzPyMe respectively. Finally, one observes that all samples exhibit a broad pore size distribution in the range of great

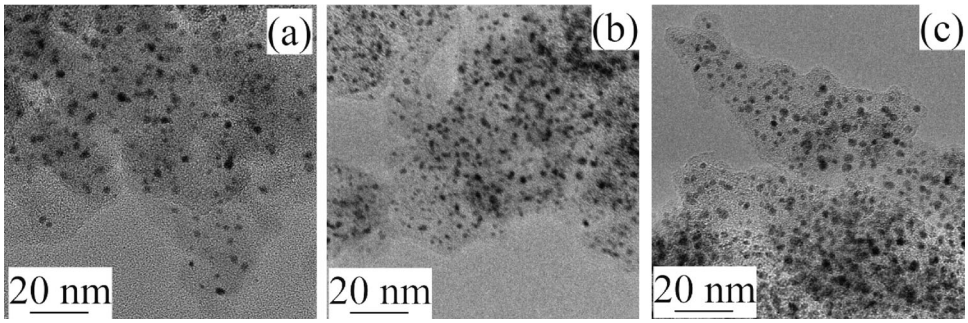

Fig. 5 TEM micrographs of samples **a** EDAPMS, **b** MS-PzPy and **c** MS-PzPyMe (350.000 ×)

meso—and macropores: this is in correlation with values of the total cumulative specific pore volume, V_v, of all the samples (Table 2). V_v, whose values evolve between 1.8 and 2.9 $cm^3\ g^{-1}$, is the pore volume obtained by addition of pore volume measured by mercury porosimetry (width < 7.5 nm), cumulative volume of mesopores of widths between 2 and 7.5 nm measured by nitrogen adsorption-desorption and volume of micropores (width < 2 nm).

Thanks to the difference in steric volume of the three silylated ligands (EDAPMS, MS-PzPy and MS-PzPyMe), the textural properties of Ni/SiO_2 cogelled xerogel catalysts show a large influence of the nature of silylated ligand on the final texture of catalysts, both before as well as after calcination and reduction steps. The specific surface area obtained by BET method, S_{BET}, presents a higher value equal to 420 and 390 $m^2\ g^{-1}$ for samples MS-PzPyMe and MS-PzPy respectively than this of sample EDAPMS (Table 2). Furthermore, in Fig. 4, the cumulative volume associated to micropores (pore size < 2 nm) is sligthly more important for samples MS-PzPy and MS-PzPyMe than for sample EDAPMS. As it is well-known that micropores (pore size < 2 nm) and small mesopores (2 nm < pore size < 10 nm) contribute essentially in S_{BET} values [24] and the silica particle sizes of Ni/SiO_2 cogelled xerogel catalysts measured by TEM measurements are equal to 13.7 nm for sample MS-PzPyMe, 15.4 nm for sample MS-PzPy and 21.2 nm for sample EDAPMS, microporosity is largely located inside silica particles. So samples MS-PzPy and MS-PzPyMe are more microporous than sample EDAPMS. This higher microporosity with the use of silylated methyl-pyrazolylpyridine ligand could be the result of its size of about 0.9 nm against sizes of about 0.8 nm for the sylilated pyrazolypyridine ligand without methyl group and of about 0.35 nm for EDAPMS (Molecular simulation with Chem3D Ultra Version 7.0). So greater repulsion between silylated pyrazolylpyridine ligand molecules could generate more spaces into silica nuclei, increasing the microporosity inside silica particles. The silica particle sizes are also smaller for samples MS-PzPyMe and MS-PzPy. This feature could also be the result of repulsion between silylated pyrazolypyridine ligand molecules, involving a small number of ligand molecules in silica nuclei.

Before calcination and reduction steps, all the samples already have high specific surface areas, S_{BET} (Table 2). When the samples are calcined in air, the organic groups are removed by thermolysis and/or pyrolysis reactions. This results in an increase in porosity and specific surface area [25]. For all samples, after calcination and reduction steps, the total cumulative pore volume, V_v, slightly increases, whereas the specific surface area, S_{BET}, strongly increases, indicating that a large percentage of micropores and small mesopores are created by the removal of the organic groups during calcination and reduction steps (Table 2).

3.2 Loading, dispersion and localization of nickel in Ni/SiO_2 cogelled xerogel catalysts

The actual nickel loading in the three Ni/SiO_2 cogelled xerogel catalysts, measured by ICP-AES, is nearly equal (0.9 wt.% in samples MS-PzPy and EDAPMS and 1.1 wt.% in sample MS-PzPyMe) to the theoretical loading of 1 wt.% of nickel. Indeed, the actual catalyst mass after drying, calcination and reduction steps, is equal to the theoretical mass. This theoretical mass (m_{th}) is calculated from:

$$m_{th} = n_{Ni} M_{Ni} + (n_{TEOS} + n_{ligand}) M_{SiO2} \quad (1)$$

where n_{Ni} is the amount of nickel complex in the gel (mmol); M_{Ni} is the nickel atomic weight; n_{TEOS} and n_{ligand} are respectively the amounts of TEOS and sylilated pyrazolypyridine or EDAPMS ligand in the gel (mmol); M_{SiO2} is the molecular weight of SiO_2, 60.085 $g\ mol^{-1}$. In this equation, it is assumed that all TEOS and ligand molecules are converted into SiO_2.

Table 2 shows the nickel particle sizes determined by TEM and H_2 chemisorption measurements.

TEM micrographs show that, in all Ni/SiO2 xerogel cogelled catalysts, the size of the nickel particles is quite homogeneous, and is about 2.8 nm (Fig. 5a–c). For all the catalysts, the mean diameter of nickel particles, d_{TEM}, is the arithmetic mean of two hundred diameters of nickel particles measured on TEM micrographs. Although TEM gives

only an 2D view, it seems that nickel particles are located inside silica matrix, like in the case of Pd/SiO_2, Ni/SiO_2, Ag/SiO_2, Cu/SiO_2, Fe_xO_y/SiO_2, Pd-Ag/SiO_2, Pd-Cu/SiO_2 and Ni-Cu/SiO_2 xerogel cogelled catalysts [5–8].

From H_2 chemisorption measurements on Ni/SiO_2 xerogel cogelled catalysts, one can calculate the nickel dispersion, D, i.e., the ratio between the number of Ni atoms located at the surface of the metal particles and the total number of Ni atoms in the catalyst, and the mean diameter of Ni crystallites, d_{chem}, as explained in [23]. Following previous studies conducted on Ni catalysts [23, 26], the chemisorption mean stoichiometry X_{Ni-H2}, that is, the mean number of Ni atoms on which one H_2 molecule is adsorbed, was chosen equal to 2. Values of D and d_{chem} are given in Table 2. For all samples, one has to note the agreement between TEM and chemisorption, assuming that all the Ni atoms located at the surface of the metal particles are accessible to H_2.

Accessibility to active sites is of crucial importance for an efficient catalytic activity. Site accessibility will naturally depend on the material structure, which is dependent on the composition of the material and on processing conditions. It is frequently found that the specific activities of metal complexes in catalytic reactions are considerably diminished when the complexes are supported on a silica gel material [27]. Such reductions in activity may arise from changes in the coordination state of the complex or other environmental influences. In many cases, however, the reduced activity may simply result from a large fraction of supported metal complexes being rendered inaccessible to solvent or external reagents. Because nickel is located inside silica particles in Ni/SiO_2 cogelled xerogel catalysts, there is a risk of inaccessibility. The values of V_v in Table 2 show that porosity remains high after drying under vacuum, although this does not prove accessibility to nickel. Nevertheless, it is observed in Table 2 that $d_{TEM} \sim d_{chem}$ for the three samples. So nickel particle sizes obtained by H_2 chemisorption measurements are related to TEM measurements, which suggests that nickel particles located inside silica particles are completely accessible.

3.3 Catalytic results for homogeneous and heterogenous Ni-based catalysts

3.3.1 Ethylene polymerization

Ethylene consumption with homogeneous catalysts is observed with all nickel complexes during 10 min. After 10 min, a black precipitate appears with each nickel complexe, which is probably a consequence of catalyst degradation. After 1 h, the reactional mixture is analyzed by gas chromatography: only oligomers are identified such as pentene isomers and no trace of polyethylene is observed.

These homogeneous catalysts present a very low activity because first, catalytic active sites generated by MAO would be unsteady. Secondly, steric cluttering generated by the ligand would be probably insufficient, which would favor β-H elimination. Indeed, it was observed that steric cluttering of ligand substituants is a very important factor for the polymerization degree and for the activity of "late transition metal" catalysts [9].

In Table 2, it is observed that after 1 h of reaction at room temperature, the mass of polyethylene is equal to 0.085 g for sample EDAPMS dried, 0.105 g for sample MS-PzPy dried and 0.520 g for sample MS-PzPyMe dried. The presence of polyethylene is determined by DSC (fusion temperature of PE = 127 °C). The production of polyethylene varies with the nature of nickel ligand and being that Ni/SiO_2 cogelled xerogel catalysts are only dried at the temperature of 150 °C under vacuum, they are already porous. It appears that the mass of produced polyethylene increases with the specific surface area, S_{BET}, and the total cumulative volume, V_v of Ni/SiO_2 xerogel cogelled catalysts. So, in this case, the heterogenization of nickel complexe allows increasing ethylene polymerization activity because the porosity of dried xerogel cogelled catalysts is high and the active sites (Ni nanoparticules) are accessible like in [16], being that there are anchored inside the silica matrix.

3.3.2 1.2-Dichloroethane hydrodechlorination

It has been shown in a previous study [7] that the very particular structure of cogelled xerogel catalysts allows to avoid diffusional limitations. So the observed rate r is equal to the intrinsic rate of the chemical reaction.

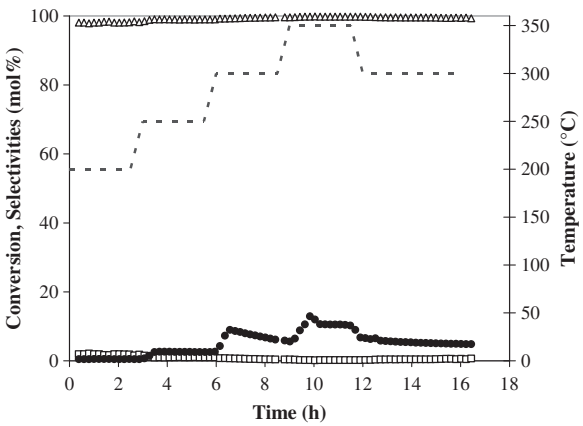

Fig. 6 *1,2*-dichloroethane hydrodechlorination over sample MS-PzPy. (●) $ClCH_2$-CH_2Cl conversion, (Δ) C_2H_6 selectivity, (□) C_2H_4 selectivity and (---) temperature

In Fig. 6, *1,2*-dichloroethane ($ClCH_2$-CH_2Cl) conversion as well as C_2H_6 (ethane) and C_2H_4 (ethylene) selectivities are given as a function of time and temperature over sample MS-PzPy, for example after calcination and reduction steps. In fact, the results are the same for the three Ni/SiO_2 cogelled xerogel catalysts because as mentioned in the experimental section, the mass of catalyst pellets (0.15 g) and Ni loading (1 wt.%) are the same in all the samples. All Ni/SiO_2 cogelled xerogel catalysts mainly produce ethane, C_2H_6, with a selectivity >97 %. The examination of conversion curves shows that a slight deactivation, which is faster when the temperature increases, is observed with all samples.

The consumption rate of *1,2*-dichloroethane, *r*, is calculated from chromatographic measurements of C_2H_6 and C_2H_4 concentrations in the reactor effluent and from the differential reactor equation that is written as follows:

$$r = \frac{F_A + F_E}{W} \tag{2}$$

where *r* is the consumption rate (mmol s^{-1} kg_{Ni}^{-1}), F_A is the molar flowrate of ethane at the reactor outlet (mmol s^{-1}), F_{A0} is the molar flowrate of ethane at the reactor inlet (mmol s^{-1}), F_E is the molar flowrate of ethylene at the reactor outlet (mmol s^{-1}), F_{E0} is the molar flowrate of ethylene at the reactor inlet (mmol s^{-1}) and *W* is the nickel mass inside the reactor (kg_{Ni}). For all calcined and reduced Ni/SiO_2 cogelled xerogel catalysts, *r* has been calculated from Eq. (2) at the temperatures of 300 °C and 350 °C and these results are presented in Table 2. It is observed that *r* is similar for all Ni/SiO_2 catalysts and increases with the temperature.

The turnover frequency (TOF), that is, the number of molecules consumed per surface nickel atom and per second, for *1,2*-dichloroethane hydrodechlorination is presented in Table 2. For Ni/SiO_2 catalysts, although a light deactivation is observed at 300 °C and 350 °C in Fig. 5, Ni dispersion of fresh catalysts is used to calculate TOF at 300 °C and 350 °C because H_2 chemisorption measurement for tested sample MS-PzPy gives a value of 30% for Ni dispersion instead of 32% for fresh sample MS-PzPy.

In Table 2, the specific consumption rate of *1,2*-dichloroethane, *r*, and the TOF increase with temperature from 300 °C to 350 °C. Furthermore, at the same temperature, values of *r* and TOF are nearly the same for all the samples. So these values are identical to those obtained for *1,2*-dichloroethane hydrodechlorination over Ni/SiO_2 cogelled xerogel catalysts synthesized with EDAS as silylated ligand [7, 28]. It seems that the *1,2*-dichloroethane hydrodechlorination over Ni/SiO_2 catalysts examined in the present study, is non-dependant of the nature of the sylilated ligand if the porosity and the specific surface area of cogelled xerogel catalysts are sufficient high, as already previously observed [7, 28].

In this work, when Ni/SiO_2 cogelled xerogel catalysts are tested for *1,2*-dichloroethane hydrodechlorination, only ethane was depicted (Fig. 6) and no ethylene was observed. Indeed, metal catalysts (Group VIII) such as Pt, Pd, Ni and Fe are very active for the following hydrodechlorination reaction [29–31]:

$$ClCH_2-CH_2Cl + 2\,H_2 \rightarrow CH_3-CH_3 + 2\,HCl \tag{3}$$

Because of the high reactivity of hydrogen on metals from Group VIII, the dechlorinated organics (in this work : $ClCH_2$–CH_2Cl) are immediately converted into the fully hydrogenated product (in this work : CH_3–CH_3). In literature, *1,2*-dichloroethane represents a reference molecule as chlorinated hydrocarbon. During hydrodechlorination, *1,2*-dichloroethane is dechlorinated by chlorination of the metal from Group VIII surface. Then the surface itself is dechlorinated by reduction with hydrogen and formed ethylene (CH_2=CH_2) is readily converted into ethane (CH_3–CH_3). It was found that platinum shows rather low activity for *1,2*-dichloroethane hydrodechlorination [32], while palladium and nickel presents a high activity for the hydrodechlorination of *1,2*-dichloroethane into ethane [31, 32].

4 Conclusions

The main purpose of the present work was to synthesize new silylated pyrazolypyridine ligands, able to form a chelate with a metal ion such as Ni^{2+} and able to react with a silica-forming reagent such as TEOS. This purpose is attained because the use of *2*-[*4*-[*3*-(trimethoxysilyl)propyl]-*3,5*-dimethyl-*1H*-pyrazol-*1*-yl]pyridine (MS-PzPy) and *2*-[*4*-[*3*-(trimethoxysilyl)propyl]-*3,5*-dimethyl-*1H*-pyrazol-*1*-yl]-*6*-methylpyridine (MS-PzPyMe) in an ethanolic solution containing nickel acetylacetonate, TEOS and an ammonia solution of 0.54 mol L^{-1} gave very homogeneous and very highly dispersed Ni/SiO_2 cogelled xerogel catalysts.

The silylated ligand has a large influence on the textural properties of Ni/SiO_2 cogelled xerogel catalysts, both before and after calcination and reduction steps. By changing the nature of the silylated ligand, *e.g.*, MS-PzPy, MS-PzPyMe or EDAPMS, textural properties such as pore volume, pore size and surface area can be tailored. For all the samples, the total cumulative pore volume, V_v, and the specific surface area, S_{BET}, increase after calcination and reduction steps, indicating that a large percentage of micropores and small mesopores are created by the removal of the organic groups during calcination and reduction steps.

In all Ni/SiO_2 xerogel cogelled catalysts, the nickel nanoparticles are located inside the silica crystallites. The

size of the nickel particles is quite homogeneous, and is about 2.8 nm (d_{TEM}) as observed by microscopy measurements. Furthermore, from H_2 chemisorption measurements, it is observed that $d_{TEM} \sim d_{chem}$ for the three samples. So nickel particle sizes obtained by H_2 chemisorption measurements are related to TEM measurements, which suggests that nickel particles located inside silica particles are completely accessible.

Homogenous nickel complexes synthesized from pyrazolylpyridine derivatives are inactive for ethylene polymerization because first, catalytic active sites generated by MAO would be unsteady. Secondly, steric cluttering generated by the ligand would be probably insufficient, which would favor β-H elimination. Heterogenous nickel-based catalysts onto silica xerogel are synthesized from pyrazolylpyridine derivatives bearing a tethered trialkoxysilyl group via a sol–gel process, yielding highly dispersed homogeneous nickel catalysts covalently bonded to silica with a finely controlled structure. The heterogenization of nickel complexe allows increasing ethylene polymerization activity.

Although nickel nanoparticles are located inside the silica crystallites, their complete accessibility, via the micropore network, is suggested. So for *1,2*-dichloroethane hydrodechlorination, the conversion of *1,2*-dichloroethane over Ni/SiO_2 cogelled xerogel catalysts is high and mainly produces ethane.

Acknowledgements SDL. is grateful to the Belgian "Fonds de la Recherche Scientifique—Fonds National de la Recherche Scientifique (F.R.S.-F.N.R.S)" for her research associate position. The authors acknowledge the Ministère de la Région Wallonne Direction Générale des Technologies, de la Recherche et de l'Energie (DG06) and the Fonds de Recherche Fondamentale Collective and the Ministère de la Communauté Française (Action de Recherche Concertée no. 00-05-265) for financial supports.

Compliance with Ethical Standards

Conflict of interest The authors declare that they have no conflict of interests.

References

1. Price PM, Clarck JH, Macquarrie DJ (2000) Modified silicas for clean technology. J Chem Soc Dalton Trans 1:101–105
2. Busca G (2014) Heterogeneous catalytic materials—Solid state chemistry, surface chemistry and catalytic behaviour. Elsevier, Amsterdam
3. Brinker CJ, Scherer GW (1990) Sol-Gel science: The physics and chemistry of sol-gel processing. Academic Press, San Diego, CA
4. Husing N, Schubert U, Mezei R, Fratzl P, Riegel B, Kiefer W, Kohler D, Mader W (1999) Formation and Structure of Gel Networks from $Si(OEt)_4/(MeO)_3Si(CH_2)_3NR'_2$ Mixtures (NR'_2 = NH_2 or $NHCH_2CH_2NH_2$). Chem Mater 11:451-457
5. Lambert S, Ferauche F, Heinrichs B, Tcherkassova N, Pirard JP, Alié C (2006) Methods for the preparation of bimetallic xerogel catalysts designed for chlorinated wastes processing. J Non-Cryst Solids 352:2751–2762
6. Lambert S, Tran KY, Arrachart G, Noville F, Henrist C, Bied C, Moreau JJE, Wong Chi Man M, Heinrichs B (2008) Tailor-made morphologies for Pd/SiO2 catalysts through sol-gel process with various silylated ligands. Microporous Mesoporous Mater 115:609–617
7. Pirard S, Mahy J, Pirard JP, Heinrichs B, Raskinet L, Lambert SD (2015) Development by the sol-gel process of highly dispersed Ni-Cu/SiO2 xerogel catalysts for selective *1,2*-dichloroethane hydrodechlorination into ethylene. Microporous Mesoporous Mater 209:197–207
8. Mahy JG, Tasseroul L, Herlitschke M, Hermann RP, Lambert SD (2016) Fe3+/iron oxide/SiO2 xerogel catalysts for p-nitrophenol degradation by photo-Fenton effects: Influence of thermal treatment on catalysts texture. Mater Today 3:464–469
9. Younkin TR, Connor EF, Henderson JI, Friedrich SK, Grubbs RH, Bansleben DA (2000) Neutral, Single-Component Nickel (II) Polyolefin Catalysts That Tolerate Heteroatoms. Science 287:460–462
10. Britovsek GJP, Bruce M, Gibson VC, Kimberley BS, Maddox PJ, Mastroianni S, McTavish SJ, Redshaw C, Solan GA, Strömberg S, White AJP, Williams DJ (1999) Iron and cobalt ethylene polymerization catalysts bearing 2,6-bis(imino) Pyridyl ligands: synthesis, structures, and polymerization studies. J Am Chem Soc 121:8728–8732
11. Wang S, Sun WH, Redshaw C (2014) Recent progress on nickel-based systems for ethylene oligo-/polymerization catalysis. J Organomet Chem 751:717–741
12. Zhang D, Meng J, Tian S (2015) Nickel cyclopentadienyl complexes as catalysts for ethylene polymerization. J Organomet Chem 798:341–346
13. Nelana SM, Darkwa J, Guzei IA, Mapolie SF (2004) Ethylene polymerization catalyzed by substituted pyrazole nickel complexes. J Organomet Chem 689:1835–1842
14. Obuah C, Omondi B, Nozaki K, Darkwa J (2014) Solvent and co-catalyst dependent pyrazolylpyridinamine and pyrazolylpyrroleamine nickel(II) catalyzed oligomerization and polymerization of ethylene. J Mol Catal A Chem 382:31–40
15. Sacco L, Lambert S, Pirard JP, Noels AF (2004) Synthesis of pyrazolylpyridine derivatives bearing a tethered alkoxysilyl group. Synthesis 5:663–665
16. Zhang L, Castillejos E, Serp P, Sun WH, Durand J (2014) Enhanced ethylene polymerization of Ni(II) complexes supported on carbon nanotubes. Catal Today 235:33–40
17. Fujii K, Ishihama Y, Sakuragi T, Ohshima MA, Kurokawa H, Miura H (2008) Heterogeneous catalysts immobilizing α-diimine nickel complexes into fluorotetrasilicic mica interlayers to prepare branched polyethylene from only ethylene. Catal Commun 10:183–186
18. Kurokawa H, Hayasaka M, Yamamoto K, Sakuragi T, Ohshima MA, Miura H (2014) Self-assembled heterogeneous late transition–metal catalysts for ethylene polymerization; New approach to simple preparation of iron and nickel complexes immobilized in clay mineral interlayer. Catal Commun 47:13–17
19. Ochedzan-Siodlak W, Dziubek K (2014) Metallocenes and post-metallocenes immobilized on ionic liquid-modified silica as catalysts for polymerization of ethylene. Appl Catal A 484:134–141
20. Nandi M, Roy P, Uyama H, Bhaumik A (2011) Functionalized mesoporous silica supported copper (II) and nickel (II) catalysts for liquid phase oxidation of olefins. Dalton Trans 40:12510–12518
21. Yates DJC, Sinfelt JH (1967) The catalytic activity of rhodium in relation to its state of dispersion. J Catal 8:348–359
22. Scholten JJF, Konvalinka JA, Beekman FW (1973) Reaction of nitrous oxide and oxygen with silver surfaces, and application to

the determination of free-silver surface areas of catalysts. J Catal 28:209–221
23. Bergeret G, Gallezot P (1997) Bimetallic catalysts. In: Ertl G, Knözinger H, Weitkamp J (eds), Handbook of heterogeneous catalysis, Wiley-VCH, Weinheim
24. Lecloux AJ (1981) Texture of catalysts. In: Anderson JR, Boudart M (ed), Catalysis: Science and technology, Vol. 2, Springer, Berlin
25. Raman NK, Anderson MT, Brinker CJ (1996) Template-Based Approaches to the Preparation of Amorphous, Nanoporous Silicas. Chem Mater 8:1682–1691
26. Ponec V, Bond GC (1995) Catalysis by metals and alloys. Elsevier, Amsterdam
27. Watton SP, Taylor CM, Kloster GM, Bowman SC (2003) Chapter 4: Coordination Complexes in Sol-Gel Silica Materials. In: Karlin KD (ed), Progress in inorganic chemistry, Vol. 51, Wiley-VCH, Weinheim
28. Lambert S, Polard JF, Pirard JP, Heinrichs B (2004) Improvement of metal dispersion in Pd/SiO2 cogelled xerogel catalysts for *1,2*-dichloroethane hydrodechlorination. Appl Catal B 50:127–140
29. Bozzelli JW, Chen YM, Chuang SSC (1992) Catalytic hydrodechlorination of 1.2-dichloroethane and trichloroethane over Rh/SiO_2 catalysts. Chem Eng Commun 115:1–11
30. Kulkarni PP, Deshmukh SS, Kovalchuk VI, d'Itri JL (1999) Hydrodechlorination of dichlorodifluoromethane on carbon-supported Group VIII noble metal catalysts. Catal Lett 61: 161–166
31. Srebowata W, Juszczyk Z, Kaszkur Z, Karpinski Z (2007) Hydrodechlorination of *1,2*-dichloroethane on active carbon supported palladium–nickel catalysts. Catal Today 124:28–35
32. Avdeev VI, Kovalchuk VI, Zhidomirov GM (2007) DFT analysis of the mechanism of *1,2*-dichloroethane dechlorination on supported Cu-Pt bimetallic catalysts. J Struct Chem 48:S171–S183